Hilbert Space Geometry of Random Matrix Eigenstates

Alexander-Georg Penner,[1] Felix von Oppen,[1] Gergely Zaránd,[2,3] and Martin R. Zirnbauer[4]
[1]*Dahlem Center for Complex Quantum Systems and Fachbereich Physik, Freie Universität Berlin, 14195 Berlin, Germany*
[2]*Exotic Quantum Phases "Momentum" Research Group, Department of Theoretical Physics, Budapest University of Technology and Economics, 1111 Budapest, Budafoki út 8, Hungary*
[3]*MTA-BME Quantum Correlations Group, Institute of Physics, Budapest University of Technology and Economics, 1111 Budapest, Budafoki út 8, Hungary*
[4]*Institut für Theoretische Physik, Universität zu Köln, Zülpicher Straße 77a, 50937 Köln, Germany*

(Received 26 March 2021; accepted 27 April 2021; published 20 May 2021)

The geometry of multiparameter families of quantum states is important in numerous contexts, including adiabatic or nonadiabatic quantum dynamics, quantum quenches, and the characterization of quantum critical points. Here, we discuss the Hilbert space geometry of eigenstates of parameter-dependent random matrix ensembles, deriving the full probability distribution of the quantum geometric tensor for the Gaussian unitary ensemble. Our analytical results give the exact joint distribution function of the Fubini-Study metric and the Berry curvature. We discuss relations to Levy stable distributions and compare our results to numerical simulations of random matrix ensembles as well as electrons in a random magnetic field.

DOI: 10.1103/PhysRevLett.126.200604

Introduction.—The geometry underlying the eigenstates of parameter-dependent quantum Hamiltonians is concisely described in terms of the quantum geometric tensor [1,2]. Its symmetric part is the Fubini-Study metric, while its antisymmetric part is the Berry curvature [3]. Both contributions to the quantum geometric tensor have important physical consequences, in particular in the context of adiabatic quantum dynamics beyond the Born-Oppenheimer approximation. When a slow system is coupled to a fast one, the symmetric and antisymmetric parts of the quantum geometric tensor govern electric and magnetic gauge forces acting on the slow system [4]. An important application of these ideas is to the semiclassical dynamics of Bloch electrons [5], where these gauge forces are at the core of anomalous Hall effects, both unquantized and quantized. In this case, each band defines a family of quantum states which is parametrized by the Bloch momenta, and it is by now well understood that the physics of electronic systems is affected by the local geometry [5] as well as the global topology of the bands [6]. In disordered or interacting systems, the magnetic fluxes threading the system in a real-space torus geometry play a role which is quite analogous to that of the Bloch momenta of noninteracting clean systems [7]. The corresponding boundary geometric tensor has been shown to provide an appropriate scaling variable for Anderson transitions, and to assume a universal probability distribution at the critical point [8]. More generally, the quantum geometric tensor is an important characteristic of quantum phase transitions [2,9].

Here, we derive the exact joint probability distribution of the quantum geometric tensor for the Gaussian unitary ensemble (GUE) of random matrix theory. The probability distribution of the quantum geometric tensor for random matrix ensembles was recently introduced by Berry and Shukla [10], extending earlier work on the Berry curvature and the fidelity susceptibility [11–14]. Berry and Shukla base their discussion on analytical results for small random matrices, which is sufficient to obtain the correct asymptotics of the distribution function, but fails to describe the bulk of the distribution for generic systems. Here, we find the exact analytical distribution for large random matrices which describe systems with delocalized dynamics in the absence of time-reversal symmetry. Large random matrices are a powerful tool to describe spectra and eigenstates of generic quantum systems [15,16] and are applicable to a remarkably diverse set of systems, including nuclear spectra [17], chaotic billiards [18], quantum chromodynamics [19], few-body chaotic quantum systems [20], disordered electron systems [21,22], nonintegrable many-body systems [23,24], and many-body localization [25–27]. Most recently, random matrix theory was instrumental in claims that quantum processors have reached the regime of quantum supremacy [28]. A central role in this argument was played by the Porter-Thomas distribution, one of only a few distribution functions in random matrix theory which are known exactly and have a simple analytical form. In view of the scarcity of exact analytical distributions in random matrix theory, it is quite remarkable that the characteristic function of the joint distribution function of the quantum geometric tensor can be obtained exactly.

Quantum geometric tensor.—We consider the eigenstates $|\tilde{n}(\boldsymbol{\lambda})\rangle$ of a multiparameter family of Hamiltonians

$H(\boldsymbol{\lambda})$ with $\boldsymbol{\lambda} = (\lambda_1, \ldots, \lambda_n)$. A metric structure associated with the parameter-dependent eigenstates can be obtained by defining the distance in Hilbert space for two states with infinitesimally different parameters as

$$ds^2 = 1 - |\langle \tilde{n}(\boldsymbol{\lambda}) | \tilde{n}(\boldsymbol{\lambda} + d\boldsymbol{\lambda}) \rangle|^2 = \sum_{\alpha\beta} \mathrm{Re} g^{(n)}_{\alpha\beta}(\boldsymbol{\lambda}) d\lambda_\alpha d\lambda_\beta. \quad (1)$$

Explicitly expanding in $d\boldsymbol{\lambda}$ yields the Hermitian quantum geometric tensor [1,2]

$$g^{(n)}_{\alpha\beta} = \langle \partial_\alpha \tilde{n} | \partial_\beta \tilde{n} \rangle - \langle \partial_\alpha \tilde{n} | \tilde{n} \rangle \langle \tilde{n} | \partial_\beta \tilde{n} \rangle. \quad (2)$$

The distance ds^2 is entirely determined by the real and symmetric part, which is also known as the quantum metric tensor. The imaginary and antisymmetric part is readily identified as the Berry curvature [3], which can be nonzero for broken time-reversal symmetry. Equation (1) indicates that the quantum geometric tensor $g^{(n)}_{\alpha\beta}$ quite generally governs the behavior of systems under quantum quenches which involve small changes of the parameters.

Following Berry and Shukla [10], we consider a two-parameter family of Hermitian $N \times N$ Hamiltonians

$$H = H_0 + x H_x + y H_y, \quad (3)$$

which depend on the real parameters x and y [29]. Evaluating the derivatives in Eq. (2) at $x = y = 0$, one can express the quantum geometric tensor in terms of the eigenenergies E_n and eigenstates $|n\rangle$ of H_0,

$$g^{(n)}_{\alpha\beta} = \sum_{m(\neq n)} \frac{\langle n | H_\alpha | m \rangle \langle m | H_\beta | n \rangle}{(E_n - E_m)^2} \quad (4)$$

with $\alpha, \beta \in \{x, y\}$.

For orientation, we first consider the distribution function of individual matrix elements of the quantum geometric tensor for an $N \times N$ matrix Hamiltonian H_0 of an integrable system whose energy eigenvalues are statistically independent. In this case, the matrix elements of the quantum geometric tensor in Eq. (4) are sums over $N - 1$ statistically independent terms, $g^{(n)}_{\alpha\beta} = \sum_{m(\neq n)} x_m$, and one expects their probability distributions $P_{\mathrm{int}}(g)$ to converge to a stable distribution in the limit $N \to \infty$. In the absence of correlations between the eigenvalues and thus of level repulsion, the distribution of the individual terms in the sum is readily seen to fall off as $1/|x|^{3/2}$ at large $|x|$ [30], with large values of $|x|$ originating from near degeneracies in the spectrum of H_0. Importantly, both the average and the variance diverge for this distribution. As a result, the sum (4) does not constitute a standard random walk, for which the central limit theorem predicts a normal distribution. Instead, the matrix elements $g^{(n)}_{\alpha\beta}$ can be viewed as Levy flights and their probability distributions are Levy stable distributions. The terms in the sum have random signs for the real and imaginary parts of off-diagonal matrix elements, but are strictly positive for diagonal elements, leading to different stable distributions. For an asymptotic $1/|x|^{3/2}$ decay at large $|x|$, one finds distributions $P_{\mathrm{int}}(g) = \int (d\xi/2\pi) e^{i\xi g} \tilde{P}_{\mathrm{int}}(\xi)$ with characteristic functions [30,31]

$$\tilde{P}_{\mathrm{int}}(\xi) = \begin{cases} e^{-\sqrt{\frac{1}{2}\gamma|\xi|}(1 + i\,\mathrm{sgn}\xi)} & \text{diagonal,} \\ e^{-\sqrt{\gamma|\xi|}} & \text{off diagonal,} \end{cases} \quad (5)$$

where γ controls the scale. Because of the $\sqrt{|\xi|}$ singularity of the characteristic function, the distributions $P_{\mathrm{int}}(g)$ fall off as $1/|g|^{3/2}$ at large $|g|$, indicating that they are dominated by individual terms in the sum (4). Physically, this broad distribution is a direct consequence of the fact that the level spacing distribution of integrable systems remains nonzero in the limit of zero spacing.

Joint distribution function for the GUE.—In generic systems, level repulsion suppresses the likelihood of small energy denominators and the distribution of matrix elements of the quantum geometric tensor decays faster. If we continue to assume that the matrix elements are dominated by individual terms in the sum (4), the tail of the distribution can be predicted on the basis of random 2×2 GUE matrices, yielding a faster asymptotic decay, $\sim 1/|g|^{5/2}$ [10]. In addition to suppressing the probability with which near degeneracies occur, level repulsion introduces correlations between the terms in the sum in Eq. (4). As a result, the distribution of the quantum geometric tensor no longer belongs to the family of Levy stable distributions. Remarkably, however, it can still be computed exactly.

We now focus on large random matrices drawn from the Gaussian unitary ensemble, which neither obeys time-reversal symmetry nor imposes any other (anti)symmetry (symmetry class A in the Altland-Zirnbauer classification [32,33]). The (Hermitian) matrices H_0, H_x, and H_y are drawn from three statistically independent GUEs,

$$P(H_0, H_x, H_y) dH_0 dH_x dH_y \propto e^{-(1/2)N \mathrm{tr}(H_0^2 + H_x^2 + H_y^2)} \prod_{i,j} d(H_0)_{ij} d(H_x)_{ij} d(H_y)_{ij}, \quad (6)$$

where the averages over H_x and H_y are introduced for convenience. We comment below on the case when the average is over H_0 only. Exploiting Hermiticity, we parametrize the quantum geometric tensor $g^{(n)}$ as $g^{(n)} = g^{(n)}_0 + \mathbf{g}^{(n)} \cdot \boldsymbol{\tau}$, where $\boldsymbol{\tau}$ denotes the vector of Pauli matrices and $g^{(n)}_0 = \frac{1}{2}\mathrm{tr} g^{(n)}$, $g^{(n)}_1 = \mathrm{Re} g^{(n)}_{yx}$, $g^{(n)}_2 = \mathrm{Im} g^{(n)}_{yx}$, and $g^{(n)}_3 = \frac{1}{2}\mathrm{tr}(\tau_3 g^{(n)})$. Notice that $g^{(n)}_2$ measures the Berry curvature and $g^{(n)}_0$, $g^{(n)}_1$, $g^{(n)}_3$ parametrize the quantum metric tensor. We can then define the joint probability distribution of the quantum geometric tensor through

$$P(g) \propto \left\langle \sum_n \delta(E_n)\delta(g_0 - g_0^{(n)})\delta(\mathbf{g} - \mathbf{g}^{(n)}) \right\rangle_{H_0,H_x,H_y}. \quad (7)$$

Here, the brackets denote the random matrix average and the first δ function ensures that we consider the quantum geometric tensor for states which are at the center of the spectrum [34].

The corresponding characteristic function defined via $P(g) = \int (d\xi_0/2\pi)[(d\boldsymbol{\xi})/(2\pi)^3] e^{i[\xi_0 g_0 + \boldsymbol{\xi}\cdot\mathbf{g}]} \tilde{P}(\xi_0, \boldsymbol{\xi})$ takes the form

$$\tilde{P}(\xi_0, \boldsymbol{\xi}) \propto \left\langle \sum_n \delta(E_n) e^{-i[\xi_0 g_0^{(n)} + \boldsymbol{\xi}\cdot\mathbf{g}^{(n)}]} \right\rangle_{H_0,H_x,H_y}. \quad (8)$$

In the limit of $N \to \infty$, the random matrix averages can be performed explicitly. We defer technical details to further below and the Supplemental Material [30], and focus first on discussing our results.

Results.—We find that the characteristic function for the quantum geometric tensor takes the exact form

$$\tilde{P}(\xi_0, \boldsymbol{\xi}) = r(X_+, X_-) e^{-(X_+ + X_-)}, \quad (9)$$

where we defined $X_\pm = \frac{1}{2}(1 + i\,\mathrm{sgn}\xi_\pm)\sqrt{\gamma|\xi_\pm|}$ in terms of $\xi_\pm = \xi_0 \pm |\boldsymbol{\xi}|$ and the rational function

$$\begin{aligned} r(a,b) = 1 &+ (a+b) + \frac{1}{3}(a^2 + 3ab + b^2) \\ &+ \frac{1}{24}\frac{a^4 + 9a^3 b + 17a^2 b^2 + 9ab^3 + b^4}{a+b} \\ &+ \frac{1}{120} ab(5a^2 + 16ab + 5b^2) \\ &+ \frac{1}{720}\frac{a^2 b^2 (13a^2 + 29ab + 13b^2)}{a+b} + \frac{1}{240} a^3 b^3 \\ &+ \frac{1}{1920}\frac{a^4 b^4}{a+b} + \frac{1}{34560}\frac{a^5 b^5}{(a+b)^2}. \end{aligned} \quad (10)$$

For the specific scalings of the GUE matrices in Eq. (6), we find $\gamma^{\mathrm{GUE}} = 4N$. Notice that $\tilde{P}(0, \mathbf{0}) = 1$, so that $P(g)$ is normalized. Equations (9) and (10) give the exact characteristic function of the distribution of the quantum geometric tensor for large GUE matrices, and are the central results of this Letter.

The characteristic functions of the distribution of the diagonal elements g_{xx} and g_{yy} are obtained from Eqs. (9) and (10) by setting $\xi_0 = \pm\xi_3 = \xi$ and $\xi_1 = \xi_2 = 0$ (see [30] for an explicit evaluation). Interestingly, the resulting exponential factor in Eq. (9) has just the same form as in Eq. (5). This also happens for the distributions of $\mathrm{Re}g_{xy}$ and the Berry curvature $\mathrm{Im}g_{xy}$, obtained by setting $\xi_1 = \xi$ or $\xi_2 = \xi$, respectively, with all other $\xi_j = 0$. Thus, it is the rational prefactor in Eq. (9) that accounts for the spectral correlations introduced by the GUE. Expanding the exponential in Eq. (9), we observe that the leading nonanalyticity of $\tilde{P}(\xi_0, \boldsymbol{\xi})$ is of the form $|\xi|^{3/2}$, which contrasts with the leading $|\xi|^{1/2}$ singularity of the characteristic function $\tilde{P}_{\mathrm{int}}(\xi)$ in Eq. (5). This implies that the GUE distribution function of the quantum geometric tensor indeed falls off as $P(g) \propto 1/|g|^{5/2}$ for large $|g|$ and thus faster than the corresponding distribution $P_{\mathrm{int}}(g) \propto 1/|g|^{3/2}$ for integrable systems, corroborating the expectation in Ref. [10].

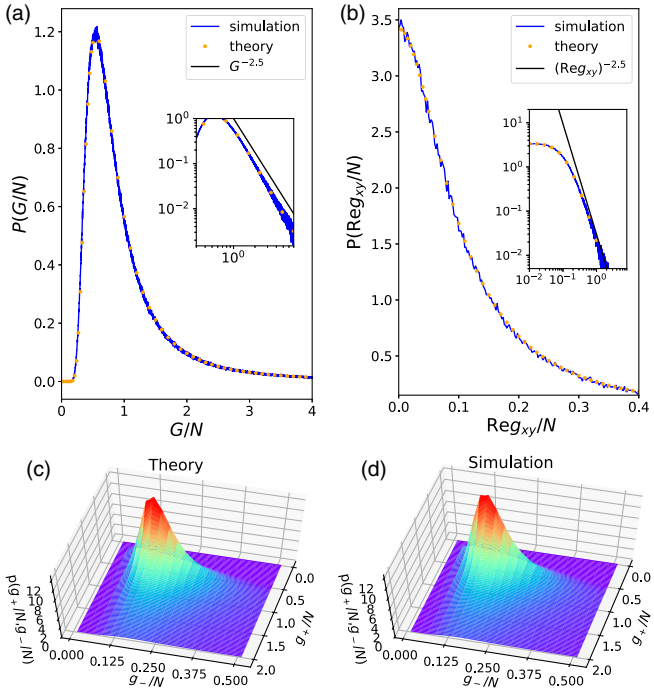

FIG. 1. Distribution functions of (a) the trace $G = \mathrm{tr}g$ and (b) the off-diagonal matrix element (real part) of the quantum geometric tensor. Numerical data for random matrices (blue lines; H_0, H_x, and H_y drawn independently from the GUE with $N = 100$, 10^6 realizations) are compared to the Fourier transform of the analytical result obtained from Eq. (9) (orange dots). (c) 3D plot of the distribution function $p(g_+, g_-)$ based on the analytical result in Eq. (12). (d) Corresponding 3D plot obtained numerically for random matrices ($N = 100$, 10^6 realizations). Insets in (a) and (b): Log-log plots emphasizing the asymptotic $1/|g|^{5/2}$ decays (black line).

Our analytical distribution functions of the quantum geometric tensor are in excellent agreement with numerical results for GUE random matrices. Figures 1(a) and 1(b) illustrate this for the distributions of $\mathrm{tr}g$ and $\mathrm{Re}g_{xy}$. We find that the off-diagonal element of the quantum metric tensor has the same distribution as the Berry curvature [11]. For a more detailed comparison to numerical simulations, we note that $P(g)$ obtained by Fourier transforming Eq. (9) depends on the quantum geometric tensor only through its eigenvalues $g_\pm = g_0 \pm |\mathbf{g}|$. Writing $g = U\mathrm{diag}[g_+, g_-]U^\dagger$, the distribution function is independent of the diagonalizing unitary matrix U, and employing a convenient

redundancy of parametrization, we define the corresponding joint eigenvalue distribution $p(g_+, g_-)$ through

$$P(g)dg = p(g_+, g_-)dg_+dg_-d\mu(U), \tag{11}$$

where $d\mu(U)$ is the invariant measure of the unitary group, with the group volume normalized to unity. We find

$$p(g_+, g_-) = -\frac{i(g_+ - g_-)}{32\pi^2}\int d\xi_+ d\xi_-(\xi_+ - \xi_-) \times \tilde{P}(\xi_0, \boldsymbol{\xi})e^{(i/2)(g_+\xi_+ + g_-\xi_-)}. \tag{12}$$

A 3D plot of this distribution in Fig. 1(c) shows excellent agreement with a numerical histogram for GUE matrices in Fig. 1(d).

Our results can also be used to compute exact and explicit distribution functions of the trace of the quantum geometric tensor for one [14] and two parameters (see Supplemental Material [30]). For larger numbers of parameters, we obtain the asymptotics at small tr$g$ in [30], which was previously considered in [10]. We also note that the GUE averages over the perturbations H_x and H_y are actually redundant in the limit of $N \to \infty$ considered above [30].

Random flux model.—The distribution function of the quantum geometric tensor is thus not very sensitive to the particular nature of the perturbation. This suggests that it applies to the large class of physical models which have been shown to display GUE random matrix correlations. Here, we illustrate this broad applicability by simulations for an appropriate Anderson model. Specifically, we consider a tight-binding model

$$H = \sum_{\langle ij\rangle} t_{ij}c_i^\dagger c_j + \sum_j \epsilon_j c_j^\dagger c_j, \tag{13}$$

with random site energies ϵ_j drawn from the interval $[-W, W]$ and hopping amplitudes $t_{ij} = e^{i\phi_{ij}}$ for the directed nearest-neighbor bonds $\langle ij\rangle$ with random phases $\phi_{ij} = -\phi_{ji}$. The random phases break time-reversal symmetry, so that the model falls into the unitary symmetry class. Placing the lattice on a torus, we thread the independent loops of the torus by fluxes ϕ_x and ϕ_y. We then compute the corresponding quantum geometric tensor $g_{\alpha\beta}$ by explicitly constructing the current operators, $J_x = \partial_{\phi_x}H$ and $J_y = \partial_{\phi_y}H$ and evaluating the expression in Eq. (4). Figure (2) shows the distribution functions of g_{xx} and Reg_{xy} for a 3D cubic lattice, where we filter the eigenstates at the center of the band and consider parameters well inside the metallic phase (moderate disorder), such that states at the band center are extended and the elastic mean free path is small compared to the system size L. The results are indeed in good agreement with the exact random matrix distribution. We observe numerically that the off-diagonal elements converge faster to the universal distribution than the diagonal elements. This difference persists for simulations of the corresponding Levy flights and is even more pronounced in simulations of a 2D random flux model. We also confirmed that the Berry curvature Img_{xy} has the same distribution as Reg_{xy} in the random flux model.

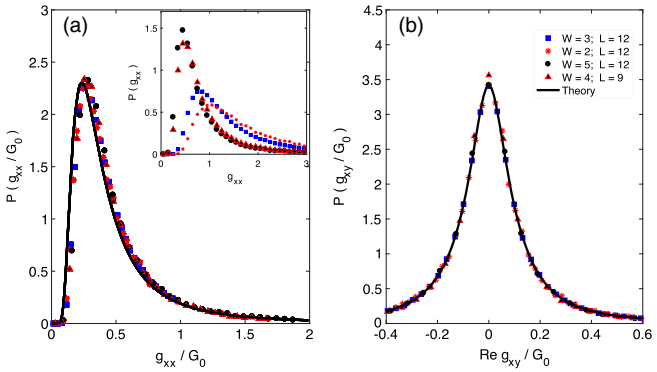

FIG. 2. Distribution functions of (a) the diagonal and (b) the off-diagonal matrix element (real part) of the quantum geometric tensor of the 3D random flux model. Numerical data [symbols; see legend in panel (b)] are compared to the analytical result obtained from Eq. (9) (full line). The inset in panel (a) shows unscaled data for g_{xx}. The data in the main panels were scaled to collapse onto a universal curve using the same set of scaling factors G_0 for g_{xx} in (a) and Re$[g_{xy}]$ in (b), namely $G_0 = 3.0395$ for $W = 3$; $L = 12$, $G_0 = 3.8685$ for $W = 2$; $L = 12$, $G_0 = 1.5760$ for $W = 5$; $L = 12$, and $G_0 = 1.7730$ for $W = 4$; $L = 9$.

Derivation.—We briefly sketch the derivation of our central result in Eq. (9), with details relegated to [30]. The averages over H_x and H_y in Eq. (8) reduce to Gaussian integrals and can be readily performed,

$$\tilde{P}(\xi_0, \boldsymbol{\xi}) \propto \left\langle \delta(E_N)\prod_{m=1}^{N-1}\frac{E_m^4}{(E_m^2 + \frac{i\xi_0}{2N})^2 + \frac{|\boldsymbol{\xi}|^2}{4N^2}}\right\rangle_{H_0}. \tag{14}$$

We reinterpret this as an average over an $(N-1)\times(N-1)$ random matrix $\tilde{H}$ with eigenvalues E_m and $m = 1, \ldots, N-1$, using the joint eigenvalue distribution of the GUE [35] (see also [36,37]). This yields

$$\tilde{P}(\xi_0, \boldsymbol{\xi}) \propto \left\langle \frac{(\det\tilde{H})^6}{\prod_{j=1}^4 \det(\tilde{H} + ia_j)}\right\rangle_{\tilde{H}}, \tag{15}$$

where the parameters a_j with $j = 1, \ldots, 4$ solve $a_j^2 = i(\xi_0 \pm |\boldsymbol{\xi}|)/2N$.

Equation (15) is now amenable to supersymmetry methods (see also Refs. [38,39] for general discussions of spectral determinants in random matrix theory). One rewrites the determinants as Gaussian integrals over $(N-1)$-dimensional vectors of commuting and anticommuting variables, performs the random matrix average over $\tilde{H}$, and employs superbosonization [40,41] to reduce the

integration over the vectors to a finite-dimensional integral. Computing this integral exactly in the $N \to \infty$ limit by the saddle-point method yields Eqs. (9) and (10), see [30] for further details.

Conclusion.—We have used supersymmetry techniques to derive the exact distribution function of the quantum geometric tensor for random matrices in the Gaussian unitary ensemble and confirmed that it applies to physical models of noninteracting electrons in the metallic regime. The matrix elements of the quantum geometric tensor can be thought of as Levy flights with correlations, and some aspects of the resulting distribution resemble corresponding Levy stable distributions. Because of the wide applicability of random matrix theory, our results promise numerous applications and extensions to specific physical systems. It would also be highly interesting to extend them to other ensembles of random matrix theory such as the Gaussian orthogonal ensemble applicable to time-reversal-invariant systems, extending earlier work [10,12–14], and beyond the limits of delocalized dynamics, both in the localized regime or at the Anderson transition, where the distribution of the quantum geometric tensor has already been considered numerically [8].

We thank Alex Altland, Christophe Mora, and Miklos Werner for insightful discussions, and Michael Berry and Pragya Shukla for helpful comments on the manuscript. This work has been supported by CRC 910 of Deutsche Forschungsgemeinschaft, by the National Research, Development and Innovation Office (NKFIH) through the Hungarian Quantum Technology National Excellence Program, Project No. 2017-1.2.1- NKP-2017-00001, by the Fund (TKP2020 IES, Grant No. BME-IE-NAT), under the auspices of the Ministry for Innovation and Technology, and the OTKA Grant No. FK 132146.

[1] J. Provost and G. Vallee, Commun. Math. Phys. **76**, 289 (1980).
[2] L. C. Venuti and P. Zanardi, Phys. Rev. Lett. **99**, 095701 (2007).
[3] M. V. Berry, Proc. R. Soc. A **392**, 45 (1984).
[4] M. V. Berry and R. Lim, J. Phys. A **23**, L655 (1990).
[5] D. Xiao, M.-C. Chang, and Q. Niu, Rev. Mod. Phys. **82**, 1959 (2010).
[6] X.-L. Qi and S.-C. Zhang, Rev. Mod. Phys. **83**, 1057 (2011).
[7] Q. Niu, D. J. Thouless, and Y.-S. Wu, Phys. Rev. B **31**, 3372 (1985).
[8] M. A. Werner, A. Brataas, F. von Oppen, and G. Zaránd, Phys. Rev. Lett. **122**, 106601 (2019).
[9] A. Carollo, D. Valenti, and B. Spagnolo, Phys. Rep. **838**, 1 (2020).
[10] M. V. Berry and P. Shukla, J. Phys. A **53**, 275202 (2020).
[11] A. Steuwer and B. D. Simons, Phys. Rev. B **57**, 9186 (1998).
[12] M. V. Berry and P. Shukla, J. Phys. A **51**, 475101 (2018).
[13] M. V. Berry and P. Shukla, J. Stat. Phys. **180**, 297 (2020).
[14] P. Sierant, A. Maksymov, M. Kuś, and J. Zakrzewski, Phys. Rev. E **99**, 050102(R) (2019).
[15] F. J. Dyson, J. Math. Phys. (N.Y.) **3**, 140 (1962).
[16] T. Guhr, A. Müller–Groeling, and H. A. Weidenmüller, Phys. Rep. **299**, 189 (1998).
[17] T. A. Brody, J. Flores, J. B. French, P. A. Mello, A. Pandey, and S. S. M. Wong, Rev. Mod. Phys. **53**, 385 (1981).
[18] M. V. Berry and M. Robnik, J. Phys. A. **19**, 649 (1986).
[19] J. Verbaarschot and T. Wettig, Annu. Rev. Nucl. Part. Sci. **50**, 343 (2000).
[20] O. Bohigas, M. J. Giannoni, and C. Schmit, Phys. Rev. Lett. **52**, 1 (1984).
[21] K. Efetov, Adv. Phys. **32**, 53 (1983).
[22] C. W. J. Beenakker, Rev. Mod. Phys. **69**, 731 (1997).
[23] D. Poilblanc, T. Ziman, J. Bellissard, F. Mila, and G. Montambaux, Europhys. Lett. **22**, 537 (1993).
[24] L. F. Santos and M. Rigol, Phys. Rev. E **81**, 036206 (2010).
[25] A. Pal and D. A. Huse, Phys. Rev. B **82**, 174411 (2010).
[26] M. Serbyn and J. E. Moore, Phys. Rev. B **93**, 041424(R) (2016).
[27] M. Filippone, P. W. Brouwer, J. Eisert, and F. von Oppen, Phys. Rev. B **94**, 201112(R) (2016).
[28] F. Arute *et al.*, Nature (London) **574**, 505 (2019).
[29] See Ref. [14] for corresponding results for a single parameter.
[30] See Supplemental Material at http://link.aps.org/supplemental/10.1103/PhysRevLett.126.200604 for technical details.
[31] J.-P. Bouchaud and A. Georges, Phys. Rep. **195**, 127 (1990).
[32] M. R. Zirnbauer, J. Math. Phys. (N.Y.) **37**, 4986 (1996).
[33] A. Altland and M. R. Zirnbauer, Phys. Rev. B **55**, 1142 (1997).
[34] We systematically ignore prefactors which can be restored from the normalization condition.
[35] F. von Oppen, Phys. Rev. Lett. **73**, 798 (1994).
[36] F. von Oppen, Phys. Rev. E **51**, 2647 (1995).
[37] Y. V. Fyodorov and H.-J. Sommers, Z. Phys. B **99**, 123 (1995).
[38] A. V. Andreev and B. D. Simons, Phys. Rev. Lett. **75**, 2304 (1995).
[39] E. Strahov and Y. V. Fyodorov, Commun. Math. Phys. **241**, 343 (2003).
[40] J. E. Bunder, K. B. Efetov, V. E. Kravtsov, O. M. Yevtushenko, and M. R. Zirnbauer, J. Stat. Phys. **129**, 809 (2007).
[41] P. Littelmann, H. J. Sommers, and M. R. Zirnbauer, Commun. Math. Phys. **283**, 343 (2008).